CORE
Metadata, citation and similar papers at core.ac.uk
Provided by AIR Universita degli studi di Milano

PHYSICAL REVIEW B **69**, 245113 (2004)

Many-body method for infinite nonperiodic systems

G. Fratesi* and G. P. Brivio†
INFM and Dipartimento di Scienza dei Materiali, Università di Milano-Bicocca, via Cozzi 53, I-20125 Milano, Italy

L. G. Molinari‡
Dipartimento di Fisica dell'Università degli Studi di Milano Via Celoria 16, I-20133 Milano, Italy
(Received 10 October 2003; revised manuscript received 11 February 2004; published 25 June 2004)

A method to implement the many-body Green function formalism in the *GW* approximation for infinite nonperiodic systems is presented. It is suitable to treat systems of known "asymptotic" properties which enter as boundary conditions, while the effects of the lower symmetry are restricted to regions of finite volume. For example, it can be applied to surfaces or localized impurities. We illustrate the method with a study of the surface of semi-infinite jellium. We report the dielectric function, the effective potential, and the electronic self-energy discussing the effects produced by the screening and by the charge density profile near the surface.

DOI: 10.1103/PhysRevB.69.245113 PACS number(s): 71.10.−w, 73.20.−r

I. INTRODUCTION

Most spectroscopic investigations (photoemission, electron energy loss, absorption, Auger decay) involve electronic excited states. The single particle picture assumes that photoemission spectra measure the bands and the density of the occupied states of the system by energy conservation. But the process is a far more complex many-body one, comprising the interaction between the photoelectron and the remaining hole plus the electronic relaxation around it. Nevertheless much progress has been achieved by calculating the spectral properties of the solid using the Kohn-Sham (KS) equation of the density functional theory (DFT). In this approach one solves a single particle self-consistent equation in which exchange correlation potentials are described by the local density approximation (LDA) or by the generalized gradient approximation (GGA). The eigenvalues of the KS equation are often interpreted as the excitation energies involved in the spectroscopic measurements, though no Koopman theorem holds in the DFT. However, this assumption may lead to severe errors. For example, it does not only strongly underestimate the gaps of semiconductors, but it also describes a Mott insulator like NiO as a metallic system.

To improve on such limitation of the DFT one could resort to methods of many-body perturbation theory. In fact they are able to account for the time dependent response of the system to an external perturbation, and give access to physical properties outside the realm of DFT, but needed for a correct description of excited states, such as quasiparticles and collective excitations.

The many-body problem was expressed by Hedin[1] as a formally exact closed set of five equations that relate the single particle Green's function, the self-energy, the polarization, the effective two-particle potential and the vertex function. The *GW* approximation[2,3] (GWA) neglects vertex corrections and reduces Hedin's system to four closed equations. The results of DFT can be used to achieve an efficient scheme of solution of the *GW* equations. In fact Dyson's equation for the exact Green function requires the input of a reference one, which in the original Hedin's formulation is the Green function for the Hartree equation. A great improvement is to use instead the Green function of the KS equation, since it includes not only the Hartree potential but also exchange and correlation effects to some local degree of correctness. This minimizes the effort for self-consistency in the evaluation of the density.

The GWA with the just mentioned input from DFT is a strategy that has been successfully applied to several systems. It combines the efficiency of the KS equation, with the use of the basic equations of many body theory, and it is able to supply excitation energies, quasiparticle lifetimes, and generalized dielectric functions. In this framework quasiparticle energies of organic semiconductors have been computed very recently.[4] The GWA can also provide reliable ground-state properties beyond the realm of applicability of current GGA functionals. Recall that the surface effective potential $V_{XC}(z)$ with the correct image tail was achieved by Eguiluz *et al.*,[5] by solving the Sham-Schlüter equation in GWA, with a slab geometry.

As already pointed out, the GWA-DFT scheme has allowed for a realistic and accurate treatment of the excited state properties of more and more complex systems of condensed matter physics.[6] Such calculations are usually confined in a finite region/supercell with periodic properties at the boundaries.[7] However, a single bulk impurity, solid surfaces, adsorbed molecules and clusters, interfaces as well as the recently investigated nanocontacts are indeed infinite or semi-infinite nonperiodic electronic systems. If their theoretical description is performed within a supercell, artificial features may occur: for example, spurious interactions, nonphysical oscillatory behaviors of the wave functions, and a discrete spectrum in which it may be difficult to isolate localized electronic states and resolve resonant ones. For example, in order to properly account for the underlying bulk band structure, a DFT evaluation of the surface dielectric function for a semi-infinite crystal, that avoids slab or supercell geometries, was recently proposed by Brodersen and Schattke.[8]

In this paper we address the problem of the description of an infinite nonperiodic system within a GWA framework. We show here that the artificial reduction of an infinite volume to a periodic one can be avoided with more transparent results.

 ©2004 The American Physical Society

Our method applies to systems (such as surfaces or localized impurities) that asymptotically in space identify with others whose relevant correlators are well studied, such as bulk crystal or vacuum. It relies on the assumption that, for any relevant correlator $F(1,2)$, there is a *finite* space region U_F outside which $F(1,2)$ cannot be distinguished from its asymptotic limit $F^{\infty}(1,2)$, within the required accuracy. This property is under control in the course of computation. It also provides a powerful tool for checking the correctness of the result, by verifying whether the correlator F matches with F^{∞} at the boundaries of U_F or not.

The virtue of this method is to replace the finite volume of the cell or slab by a finite effective volume U_F with boundary conditions that are intrinsic to the system. The property that "asymptotic" regions actually determine an effective region U_F of finite volume for the computation is connected with the principle of nearsightedness recently introduced by Kohn.[9,10] It states that the local electronic structure near a point $\mathbf{r}$, while requiring in principle the knowledge of the density (or the effective potential) everywhere, is largely determined by the potential near $\mathbf{r}$.

This strategy to deal with nonperiodic unbounded systems is of course not restricted to the GWA, which is here described in detail. Recent improvements, that include vertex corrections arising from appropriate approximations of the Bethe-Salpeter kernel, should also benefit from this method.[6]

In Sec. II we shall present the main points of the GWA to set the stage for further developments. Section III outlines the method. Two main ingredients are the embedding approach for the zeroth order Green function, which guarantees that the properties of the infinite nonperiodic system are taken correctly into account, and a lemma for the inversion of infinite matrices. The application to the semi-infinite jellium is worked out in Sec. IV. Because of its generality, the jellium surface is currently used as a bench mark system to evaluate many-body features.[11] This extension of the GWA to the semi-infinite jellium can provide further data especially on how many-body properties affect the spectral ones for a true continuum. In this respect we calculate the dielectric function, the effective potential, the self-energy, and the spectral weight function.[12] Finally Sec. V is devoted to the conclusions.

II. THE *GW* APPROXIMATION

We wish to carry out a many-body treatment of an infinite non periodic system in the GWA. In this section we recall the basic properties and the equations of the GWA. To be specific, we consider a system of electrons with Coulomb interaction $v(\mathbf{r},\mathbf{r}')$, in a static external potential $V_{\mathrm{ext}}(\mathbf{r})$ that couples to the density $\hat{n}(\mathbf{r})$, described by the Hamiltonian

$$\hat{H} = \sum_i \frac{1}{2}\hat{\mathbf{p}}_i^2 + \sum_{i<j} v(\hat{\mathbf{r}}_i,\hat{\mathbf{r}}_j) + \int d\mathbf{r} V_{\mathrm{ext}}(\mathbf{r})\hat{n}(\mathbf{r}). \tag{1}$$

Atomic units ($a_0 = 0.529$ Å, 1 Hartree $= 27.2$ eV) are used throughout this paper.

Since we are not interested in a spin-polarized phase, we consider a ground state with equal occupations for spin. The fermionic correlators are then proportional to the unit spin matrix. Two-point correlators are time translation invariant and will be considered in frequency space.

The GWA Refs. 2 and 3 is a self-consistent scheme that originates from truncating the exact closed set of five Hedin's equations for the five basic quantities: Green function G, self-energy Σ, effective potential W, polarization P, and vertex function Γ. This simplification is achieved by neglecting all vertex corrections.

The computational effort is reduced if one makes reference to the Green function G_0 that solves the Kohn-Sham equation

$$\left[\omega + \frac{1}{2}\nabla_{\mathbf{r}}^2 - V_{\mathrm{KS}}(\mathbf{r})\right] G_0(\mathbf{r},\mathbf{r}',\omega) = \delta(\mathbf{r}-\mathbf{r}'), \tag{2}$$

$$V_{\mathrm{KS}}(\mathbf{r}) = V_H(\mathbf{r}) + V_{\mathrm{ext}}(\mathbf{r}) + V_{\mathrm{XC}}(\mathbf{r}). \tag{3}$$

The Hartree potential $V_H(\mathbf{r}) = \int d\mathbf{r}' v(\mathbf{r},\mathbf{r}') n(\mathbf{r}')$ and the exchange-correlation potential $V_{\mathrm{XC}}(\mathbf{r})$ contain the unknown density of the interacting system, which is to be found self-consistently by the relation $n(\mathbf{r}) = -2i\int d\omega G_0(\mathbf{r},\mathbf{r},\omega)e^{i\omega\eta}$, where $\eta \to 0^+$. Once the reference Green function G_0 is computed by Eq. (2), in the GWA one usually proceeds by evaluating first the (ring) diagram for the polarization as

$$P_0(\mathbf{r}_1,\mathbf{r}_2,\omega) = -2i\int_{-\infty}^{+\infty} \frac{d\omega'}{2\pi} e^{i\omega'\eta} G_0(\mathbf{r}_1,\mathbf{r}_2,\omega + \omega') G_0(\mathbf{r}_2,\mathbf{r}_1,\omega'). \tag{4}$$

The effective potential is next obtained by solving the following Dyson's equation:

$$W_0(\mathbf{r}_1,\mathbf{r}_2,\omega) = v(\mathbf{r}_1,\mathbf{r}_2) + \int d\mathbf{r}_3 \int d\mathbf{r}_4 v(\mathbf{r}_1,\mathbf{r}_3) P_0(\mathbf{r}_3,\mathbf{r}_4,\omega) W_0(\mathbf{r}_4,\mathbf{r}_2,\omega). \tag{5}$$

The exchange correlation self-energy (we drop the subscript 0 for sake of simplicity) is given by

$$\Sigma_{\mathrm{XC}}(\mathbf{r}_1,\mathbf{r}_2,\omega) = i\int_{-\infty}^{+\infty} \frac{d\omega'}{2\pi} e^{i\omega'\eta} G_0(\mathbf{r}_1,\mathbf{r}_2,\omega + \omega') W_0(\mathbf{r}_2,\mathbf{r}_1,\omega'). \tag{6}$$

Finally we write down the Dyson equation for G_1:

$$G_1(\mathbf{r}_1,\mathbf{r}_2,\omega) = G_0(\mathbf{r}_1,\mathbf{r}_2,\omega) + \int d\mathbf{r}_3 \int d\mathbf{r}_4 G_0(\mathbf{r}_1,\mathbf{r}_3,\omega) \times [\Sigma_{\mathrm{XC}}(\mathbf{r}_3,\mathbf{r}_4,\omega) - V_{\mathrm{XC}}(\mathbf{r}_3)\delta(\mathbf{r}_3 - \mathbf{r}_4)] G_1(\mathbf{r}_4,\mathbf{r}_2,\omega). \tag{7}$$

In principle, one should iterate the cycle from Eq. (4) to Eq. (7) for self-consistency, by inserting G_1 in Eq. (4). Experience with the homogeneous electron gas (HEG) has shown that spectral properties are better reproduced by a first-iteration calculation rather than by a self-consistent one.[13]

III. THE METHOD

In this section we present a method to evaluate the basic many body correlators for an infinite nonperiodic system in the KS+GWA scheme, outlined in the previous section. For periodic systems, the calculations can be restricted to a finite volume (e.g., the unit cell of a lattice crystal) with suitable boundary conditions. The present method implements the same procedure for infinite systems without such a periodicity in a viable way. A weaker hypothesis is used: along the directions of broken symmetry any correlator F can be approximated by the known F^{∞} except for a finite length. Hence the calculation is carried on only in a finite volume, with boundary conditions determined by the "asymptotic properties of the system," i.e., by F^{∞}. A direct space representation will be privileged in the directions where periodicity is absent.

In developing the method, we need two technical tools, which are provided in the Appendixes. The first in Appendix A is the proof of a very useful lemma for the inversion of infinite matrices, which permits to solve the Dyson equations for W_0 and G_1 in Eqs. (5) and (7), respectively. The second in Appendix B is the standard analytic continuation in the complex plane of frequency integrals.

A. The embedding method

To start, the Green function G_0 of the KS Eq. (2) is needed. For an infinite non periodic system, we have to resort to a method which retains the advantages of the KS approach without introducing any fictitious boundary conditions. The Green function embedding approach[14–16] fulfils those conditions. Such a tool has been applied successfully to the study of infinite systems without 3D periodicity, such as bulk impurities, surfaces and adsorbates.[7] Its great advantage compared to the slab and the supercell techniques is to provide a truly continuous density of states and the correct asymptotic behavior of all physical quantities.

In the embedding method, which is here briefly sketched, space divides into a finite region V and one (or many) region V' where, to the required accuracy, the asymptotic regime is valid. The KS equation (2) in $V \cup V'$ is rewritten as an equation for the finite region V only. The effect of V' appears as a surface term that adds to the KS potential. The modified KS equation, for $\mathbf{r}$ and $\mathbf{r}'$ in V reads

$$[\omega - H_{\mathrm{KS}}(\mathbf{r})]G_0(\mathbf{r},\mathbf{r}',\omega) - \int_S d^2\mathbf{r}'' U_S(\mathbf{r},\mathbf{r}'',\omega)G_0(\mathbf{r}'',\mathbf{r}',\omega) = \delta(\mathbf{r}-\mathbf{r}'), \tag{8}$$

where S is the boundary of V. The kernel $U_S(\mathbf{r},\mathbf{r}',\omega)$ is nonzero only for $\mathbf{r},\mathbf{r}' \in S$, and it is constructed from the Green function of the KS equation in the asymptotic region V', with Neumann boundary conditions on S.

We emphasize that the embedding method is formally exact and that G_0 exhibits the truly continuous spectrum of the system. Being the solution of Eq. (8), G_0 is known only for $\mathbf{r}$ and $\mathbf{r}'$ both in V. When the value of G_0 for one or both arguments outside V is required, it can be obtained with the "matching Green function" method.[17]

B. The polarization

To compute the polarization P_0 in Eq. (4) numerically, we can take advantage of the known function P_0^{∞}, that corresponds to the asymptotic limit of P_0 continued into the region of interest, and it is evaluated by means of the KS solution G_0^{∞}. If we set $G_0 = G_0^{\infty} + \Delta G_0$, the ring integral yields P_0^{∞} and better converging corrections, owing to the rapid decay of $\Delta G_0 = G_0 - G_0^{\infty}$ as $|\omega| \to \infty$. Because of the nonanalytic behavior of the Green function close to the real axis, it is convenient to compute the polarization with the change of contour described in Appendix B. Since the spatial dependence is not involved in the computation of the polarization, such dependence amounts to that of G_0 in the same region.

C. The effective potential

The effective (dressed) potential, solution of the Dyson equation (5) physically involves ε^{-1}, the functional inverse of the nonlocal dielectric function ε, and it is formally given by the integral

$$W_0(\mathbf{r}_1,\mathbf{r}_2,\omega) = \int d\mathbf{r}_3 \varepsilon^{-1}(\mathbf{r}_1,\mathbf{r}_3,\omega) v(\mathbf{r}_3,\mathbf{r}_2), \tag{9}$$

where

$$\varepsilon(\mathbf{r}_1,\mathbf{r}_2,\omega) = \delta(\mathbf{r}_1-\mathbf{r}_2) - \int d\mathbf{r}_3 v(\mathbf{r}_1,\mathbf{r}_3) P_0(\mathbf{r}_3,\mathbf{r}_2,\omega). \tag{10}$$

The decay properties of the polarization P_0 as $|\mathbf{r}_1-\mathbf{r}_2| \to \infty$ imply that Eq. (10) can be evaluated numerically by introducing cutoffs for the integration variable $\mathbf{r}_3$. The inverse dielectric function is formally defined by

$$\int d\mathbf{r}_3 \ \varepsilon(\mathbf{r}_1,\mathbf{r}_3,\omega)\varepsilon^{-1}(\mathbf{r}_3,\mathbf{r}_2,\omega) = \delta(\mathbf{r}_1-\mathbf{r}_2). \tag{11}$$

The inversion of the matrix ε on an unbounded region is not a feasible numerical calculation. However, we only need evaluate ε^{-1} in a finite region U_ε outside which the asymptotic regime holds. Since in ordinary systems the effective interaction between electrons far apart decays to zero as the distance increases, Eq. (9) implies that also $\varepsilon^{-1}(\mathbf{r}_1,\mathbf{r}_2)$ goes to zero as $|\mathbf{r}_1-\mathbf{r}_2| \to \infty$. So we can use the Lemma proven in the Appendix A and restrict the integration in Eq. (11) to a finite region $V_\varepsilon, U_\varepsilon \subset V_\varepsilon$, still obtaining correct values of $\varepsilon^{-1}(\mathbf{r}_1,\mathbf{r}_2)$ for $\mathbf{r}_1,\mathbf{r}_2 \in U_\varepsilon$. An expansion over a discrete basis set is now possible, leading the problem to an ordinary matrix inversion. The size of the region V_ε is a numerical parameter, and convergence in the resulting ε^{-1} must be checked. With this purpose, a localized basis set is more convenient.

The effective potential can now be evaluated from Eq. (9). We only remark that the frequency argument ω is fixed, so W_0 is computed just for the same frequency values as those for the polarization, i.e., ω purely imaginary as discussed in Appendix B. The size of the minimal V_ε depends on the frequency. However, being ω imaginary, the region chosen for $\omega=0$ can be safely used for all other frequencies. Finally

we note that the assertion that $\varepsilon^{-1}(\mathbf{r}_1,\mathbf{r}_2)\to 0$ as $|\mathbf{r}_1-\mathbf{r}_2|\to\infty$ before ε^{-1} is actually evaluated does not pose conceptual difficulties: the decay to zero has in fact to be checked for the known function $(\varepsilon^{\infty})^{-1}$.

D. The self-energy

It is customary to split the self-energy into the sum of the exchange $\Sigma_X=iGv$ and the correlation term $\Sigma_C=iG(W-v)$. The evaluation of the exchange term poses no problem: the frequency integration sums over the occupied KS states, and can be performed analytically if the spectrum is discrete. In unbounded systems, the spectrum is generally continuous [G_0 is the solution of Eq. (8)], and the sum is replaced by an integral to be performed numerically. The change of contour, described in Appendix B, proves useful, together with the information that we shall be dealing with systems in which there are no KS states below the bottom of the band.

The main contribution to the correlation term is Σ_C^{∞}. Therefore, in the evaluation of the integral, one can use the splitting $G_0=G_0^{\infty}+\Delta G_0$, to obtain a leading asymptotic term plus a correction due to the inhomogeneity, as in Sec. III B for the polarization.

E. The Green function

The Dyson equation for G_1 [Eq. (7)] is formally the same as the Dyson equation for W_0 [Eq. (5)] once G_1, $\Sigma_{XC}-V_{XC}$ and G_0 are identified with W_0, P_0, and v, respectively. Therefore we define the function $\epsilon_{XC}(\mathbf{r}_1,\mathbf{r}_2,\omega)$, which is analogous to the dielectric function

$$\epsilon_{XC}(\mathbf{r}_1,\mathbf{r}_2,\omega)=\delta(\mathbf{r}_1-\mathbf{r}_2)-\int d\mathbf{r}_3 G_0(\mathbf{r}_1,\mathbf{r}_3,\omega)\times[\Sigma_{XC}(\mathbf{r}_3,\mathbf{r}_2,\omega)-V_{XC}(\mathbf{r}_2)\delta(\mathbf{r}_3-\mathbf{r}_2)]. \tag{12}$$

Even with the these strong analogies, ϵ_{XC} presents a striking difference with ε: the decay of ϵ_{XC} is linked to the one of G_0, which in turn varies according to the dimensionality of the system. As a consequence, $\epsilon_{XC}(\mathbf{r},\mathbf{r}')$ may not go to zero as $|\mathbf{r}-\mathbf{r}'|$ goes to infinity, thus not satisfying the hypothesis of the lemma in Appendix A. To make G_0 decay as $|\mathbf{r}-\mathbf{r}'|\to\infty$ (which implies the same property for ϵ_{XC}), it is convenient to solve Eq. (12) at a complex frequency $\omega+i\Delta$. The choice of the real quantity Δ depends on a compromise: if it is too small, the decay of G_0 is very slow and a large region of inversion of ϵ_{XC} is needed; if it is too large, the structures on the real frequency axis we are interested in are broadened—in fact Δ plays the role of resolution. The final result of the calculation, the interacting Green function, is thus evaluated on a translated frequency axis $\omega+i\Delta$. Analytical continuation improves the resolution: first, the values of G are fitted with a rational function, then the expression is continued to the real frequency axis.

IV. SEMI-INFINITE JELLIUM

A. Basics

In this section we illustrate the application of the method to semi-infinite jellium.[18] Semi-infinite jellium is a neutral system of dynamical electrons in a background of uniform positive charge density $n=1/(4\pi r_s^3/3)$ in the half-space $z\leqslant 0$. In the half-space $z>0$ there is no positive charge. We choose the value of r_s to give an electron density equal to that of aluminium ($r_s=2.07a_0$). The exchange-correlation potential in the KS equation is taken in the LDA.[16]

The system is invariant under translations parallel to the surface. Hence the wave vector parallel to the surface $\mathbf{k}_{\parallel}$ is a good quantum number. It is important to observe that since the solid is semi-infinite, the wave vector k_z may take any real value. So we are able to deal with truly continuous densities of states, also for a fixed $\mathbf{k}_{\parallel}$. Owing to this property any arbitrary small energy excitations are allowed by semi-infinite jellium, which results in a correct description of the response functions computed at the Fermi level.[19] A jellium slab calculation, which can only work out a discrete spectrum (i.e., a nonphysical quantized set of k_z wave vectors), cannot deal with infinitesimal excitations.

The study of semi-infinite jellium is basically one-dimensional and satisfies the requirements of applicability of our method. The perturbation induced by the jellium edge is localized near the surface. At a distance of few r_s inside the solid, the properties of the system approach those of the infinite, homogeneous electron gas (HEG). Many-body results for the HEG in the *GW* approximation are well known in the literature.[13] If we indicate by $F_n^{HEG}(k,\omega)$ the correlator F evaluated for a HEG of density n, the bulk and vacuum limits of F are

$$F_{B,V}^{\infty}(z,z',k_{\parallel},\omega)=\int\frac{dk_z}{2\pi}e^{ik_z(z-z')}F_{n_B,n_V}^{HEG}(\sqrt{\mathbf{k}_{\parallel}^2+k_z^2},\omega). \tag{13}$$

Therefore we need evaluate a correlator F only on a limited interval of the z axis $U_F=[z_B,z_V]$. Care must be taken when F is evaluated at z and z' in different regions of space, e.g., z in bulk and z' in vacuum. However, the important property $F(z,z')\to 0$ when $|z-z'|\to\infty$ guarantees that when z is in bulk and z' in vacuum the functions $F_B(z,z')$ and $F_V(z,z')$ are both zero to the desired accuracy, if $|z_B-z_V|$ is large enough.

The dependence of F on its four arguments $(z,z',k_{\parallel},\omega)$ is in principle continuous. Numerically, we stored the information about F on a four dimensional discrete mesh. Intermediate values, when necessary, are obtained with interpolation algorithms. For z and z' meshes, natural limit values are given by z_B and z_V. Cutoffs for $k_{\parallel}$ and ω can be fixed since $F\to 0$ when $k_{\parallel}\to\infty$ or $|\omega|\to\infty$. Different meshes have to be chosen for different functions.

B. Results

We consider the polarization P_0 first. The parallel wave vector convolution in Eq. (4) does not pose numerical difficulties. Regarding the frequency convolution, the factor $e^{i\omega'\eta}$ is necessary for the convergence of the integral. In fact the Green function $G_0(\omega)$ approaches zero as $|\omega|^{-1/2}$ as $|\omega|\to\infty$, as it can easily be verified for the HEG Green function. We follow the treatment of Sec. III B, and write $G_0=G^{HEG}$

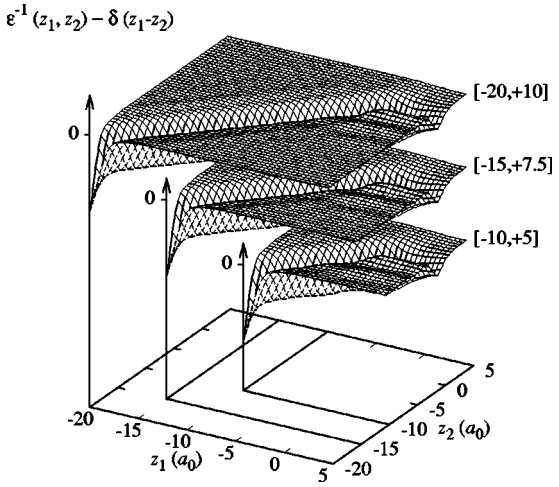

FIG. 1. Values of $\varepsilon^{-1}(z_1,z_2)-\delta(z_1-z_2)$ for different inverting regions $V_\varepsilon=[L_B,L_V]$. Here, $r_s=2.07a_0$, $\omega=0$, and $k_\parallel=0.2k_F$, k_F being the Fermi wave vector.

$+\Delta G$. The leading term, $G^{\mathrm{HEG}}G^{\mathrm{HEG}}$, gives P^{HEG}, the others can be evaluated numerically, because $\Delta G(\omega)$ goes to zero as $|\omega|^{-3/2}$ when $|\omega|\to\infty$.

The same procedure can be adopted in the calculation of the correlation term of the self-energy, i.e., $\Sigma_C=iG(W-v)$. However, the difference $W-v$ already decays fast enough to ensure convergence.

Omitting the dependence on $k_\parallel$ and ω, we rewrite Dyson's equation (9) for W_0 as

$$W_0(z_1,z_2)=\int dz_3\ \varepsilon^{-1}(z_1,z_3)v(|z_3-z_2|),$$

where ε^{-1} is defined by the inversion of ε over the whole z axis. Since the asymptotic value of ε^{-1} are known from the HEG, this function has to be evaluated on a finite interval $U_\varepsilon=[z_B,z_V]$. We exploit the lemma in Appendix A and restrict the inversion to the finite interval $V_\varepsilon=[L_B,L_V]$, $U_\varepsilon\subset V_\varepsilon$. Correct values of $\varepsilon^{-1}(z_1,z_2)$ for $z_1,z_2\in U_\varepsilon$ are obtained if L_B and L_V are conveniently large. This concept is graphically presented in Fig. 1, where we show ε^{-1} for different values of L_B and L_V. The negative peak for $z_1,z_2=L_B$ (on the left of each plot) represents a spurious feature introduced when the region of integration is restricted to a finite interval. This behavior is located at the boundaries of V_ε regardless of its size, as $\varepsilon^{-1}(z_1,z_2)$ is different from zero only for values of z_2 close to z_1. Hence the interval V_ε has to be only slightly larger than U_ε. For the values described in Fig. 1, if $z_B=-15a_0$, the choice $L_B=-20a_0$ is already an accurate one. A similar discussion has to be done with respect to L_V, but in this case the spurious peak is much smaller.

We discuss the calculated effective potential by displaying first the contour levels of the difference between the effective and bare interaction W_0-v in the z_1,z_2 plane in Fig. 2. This is also a convenient test to check the convergence of the inversion procedure of the dielectric function, in terms of the resulting W_0. The HEG levels (thinner lines) of W_0-v are also reported. The agreement is excellent when z_1 and z_2

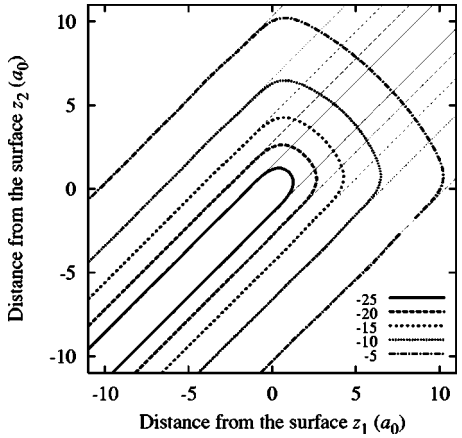

FIG. 2. Contour levels of $W_0(z_1,z_2,k_\parallel,\omega)-v(|z_1-z_2|,k_\parallel)$ in the z_1,z_2 plane. Thick curves: semi-infinite jellium. Thin curves: HEG of equal density. Here $r_s=2.07a_0$, $\omega=0$, and $k_\parallel=0.2k_F$.

approach bulk. As we move into the vacuum, W_0-v correctly goes to zero. Next we consider the effective potential W_0 in the more intuitive direct space representation $(\mathbf{r}_1,\mathbf{r}_2,\omega)$ obtained by anti-FT with respect to $\mathbf{k}_\parallel$. For simplicity, we limit our discussion to the static case ($\omega=0$) and consider collinear points on the normal to the surface ($\mathbf{r}_{1\parallel}=\mathbf{r}_{2\parallel}$). Figure 3 shows W_0 as a function of z from bulk to vacuum: W_0 is similar to a Yukawa screened potential for z_1 and z_2 in bulk, and it coincides with the bare Coulomb interaction for z_1 and z_2 in vacuum. Some intermediate values are shown: for z_1 fixed near the surface, W_0 is no longer a symmetric function of z_2 with respect to z_1, as the screening is inhomogeneous.

In Fig. 4 we report the contour levels of the self-energy evaluated at $k_\parallel=0$ and $\omega=\mu$, μ being the chemical potential. A particular feature in the near-surface region is the "Arabian" shape of the contours levels. This is an effect of the inhomogeneous density at the metal surface: when z_1 and z_2 lie outside jellium, the self-energy, as $|z_1-z_2|$ increases, decreases in a slower way than in bulk owing to lower screening. This particular feature of the surface cannot be reproduced by models based on an average density, as the one proposed in Ref. 20 and successfully tested for bulk materi-

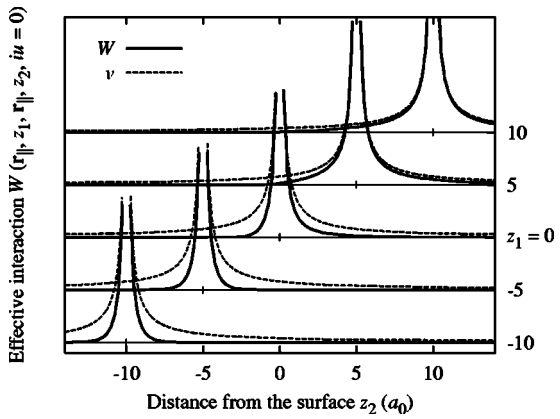

FIG. 3. Effective and bare Coulomb interaction near the jellium surface for points aligned on the normal. Here $\omega=0$. $r_s=2.07a_0$.

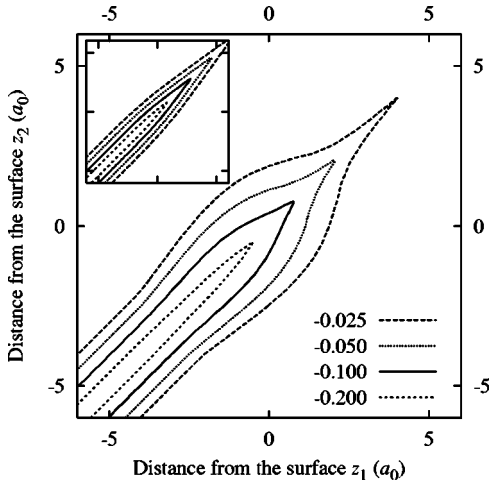

FIG. 4. Self-energy $\Sigma_{XC}(z_1,z_2,k_\parallel,\omega)$ for $r_s=2.07\ a_0$, $k_\parallel=0$, and $\omega=\mu$. Inset: model in Ref. 20.

als (see the inset in Fig. 4). Since the origin of this phenomenon is the inhomogeneity of the surface density and not the continuous spectrum description, a thick enough slab should reproduce the same density and hence the same findings.

The spectral properties of the system are the final goal of this method. They can be accessed from the many-body spectral weight function

$$A(z,\mathbf{k}_\parallel,\omega) = -\frac{1}{\pi}\mathrm{Im}\ G(z,z,\mathbf{k}_\parallel,\omega)\mathrm{sgn}(\omega-\mu). \qquad (14)$$

As discussed in Sec. III E, to solve Dyson's Eq. (7) for the Green function G, one identifies the kernel of ϵ_{XC} of Eq. (12) with ε and adds an imaginary part $i\Delta$ to the frequency to make $\epsilon^{-1}_{XC}(z_1,z_2)$ decay to zero as $|z_1-z_2|$ goes to infinity, thus satisfying the hypothesis of the lemma in Appendix A. Then the same procedure as just shown for the effective potential follows. We experienced that an interval V_ϵ about $100a_0$ wide was needed for a value of Δ of about 0.05 Hartree, in order to describe the surface region correctly.

The spectral weight function in Eq. (14) provides an estimate of the quasiparticle amplitude and is directly related to a variety of experiments such as photoemission spectroscopies,[21] and scanning tunneling microscopy.[22] The integral in $\mathbf{k}_\parallel$ gives the local density of states (LDOS)

$$\sigma(z,\omega) = \int \frac{d^2\mathbf{k}_\parallel}{(2\pi)^2}A(z,\mathbf{k}_\parallel,\omega). \qquad (15)$$

The evaluation of the LDOS of semi-infinite jellium in this framework demonstrates the presence at the surface of a broad image-potential induced (IPI) resonance, which emerges sharply when results are compared to DFT-LDA ones. We stress that an IPI resonance width can only be obtained by a many-body approach like ours which takes into account the semi-infinite character of the solid. We refer to Ref. 12 for the results and a detailed discussion on this topic.

V. CONCLUSIONS

We have presented a method to investigate infinite nonperiodic systems in the framework of the GWA. Calculations can be performed in finite regions, without introducing nonphysical boundary conditions, such as confining barriers (the slab approach) or a 3D fictitious periodicity (the supercell one). In such systems (e.g., a solid with a surface) densities of states are continuous, and while really discrete states may exist inside gaps, other ones become resonances when they do overlap in energy with a continuum band. The proposed method is particularly suitable for the description of these systems. In fact on the one side the embedding approach, which allows for calculating a truly continuous density of states, includes automatically the hybridization between bulk and surface states. On the other many-body effects, whose treatment is needed for excited states or image potential ones, are accounted for at the GWA level.

On the contrary a DFT slab calculation of such systems (e.g., in the LDA or GGA) is only able to work out a spectral weight constituted by delta functions, one for each discrete eigenstate, while the real structure of the spectrum may be in general more complicate as just outlined. The GWA correction cannot amend by itself this result, but only determine a broadening of quasiparticle states (plus eventually minor additional structures) due to many-body correlations. This broadening, which can be evaluated in first approximation by taking the average value of the self-energy over the DFT state, may be much smaller than that due to hybridization effects, as it is the case for IPI resonances.

In this paper we have also extensively investigated semi-infinite jellium by our approach. We have illustrated the bulk-to-vacuum transition of the many-body electron gas properties. By comparing the LDA and GWA density of states, this method has been able to identify an image potential surface resonance of large width.[12] Extension of this approach to semi-infinite realistic surfaces[23] could bring a wealth of accurate data on the spectral properties of surfaces and adsorbates, especially regarding the excited states.

ACKNOWLEDGMENTS

We would like to thank M. I. Trioni and G. Onida for useful discussions. This work was supported by the Italian MIUR through Grant No. 2001021128.

APPENDIX A: INVERSION OF INFINITE MATRICES

Consider the equations defining the inverse of a matrix A on two different volumes Ω and V, with $V\subset\Omega$:

$$\int_\Omega d\mathbf{r}_3 A(\mathbf{r}_1,\mathbf{r}_3)A^{-1}_\Omega(\mathbf{r}_3,\mathbf{r}_2) = \delta(\mathbf{r}_1,\mathbf{r}_2), \quad \mathbf{r}_1,\mathbf{r}_2\in\Omega, \qquad (A1)$$

$$\int_V d\mathbf{r}_3 A(\mathbf{r}_1,\mathbf{r}_3)A^{-1}_V(\mathbf{r}_3,\mathbf{r}_2) = \delta(\mathbf{r}_1,\mathbf{r}_2), \quad \mathbf{r}_1,\mathbf{r}_2\in V. \qquad (A2)$$

In general A^{-1}_V is different from the restriction of A^{-1}_Ω in V. However, the following lemma gives a condition for the two

matrices to coincide on a smaller subset $U \subset V \subset \Omega$.

Lemma. If $A_\Omega^{-1}(\mathbf{r}_1,\mathbf{r}_2)=0$ for all $\mathbf{r}_1 \in \Omega - V$ and $\mathbf{r}_2 \in U$, then $A_\Omega^{-1}(\mathbf{r}_1,\mathbf{r}_2)=A_V^{-1}(\mathbf{r}_1,\mathbf{r}_2)$ for all $\mathbf{r}_1,\mathbf{r}_2 \in U$.

Proof. consider Eq. (A1) for $\mathbf{r}_1 \in V$ and $\mathbf{r}_2 \in U$, multiply it by $A_V^{-1}(\mathbf{r}_4,\mathbf{r}_1)$ and integrate in $\mathbf{r}_1$ over V:

$$\int_V d\mathbf{r}_1 A_V^{-1}(\mathbf{r}_4,\mathbf{r}_1)\int_\Omega d\mathbf{r}_3 A(\mathbf{r}_1,\mathbf{r}_3)A_\Omega^{-1}(\mathbf{r}_3,\mathbf{r}_2) = A_V^{-1}(\mathbf{r}_4,\mathbf{r}_2).$$

The integral in $\mathbf{r}_3$ over Ω is split into an integral on V and on $\Omega - V$. The first integral yields $A_\Omega^{-1}(\mathbf{r}_4,\mathbf{r}_2)$, the latter vanishes because $A_\Omega^{-1}(\mathbf{r}_1,\mathbf{r}_2)=0$ for $\mathbf{r}_1 \in \Omega - V$ and $\mathbf{r}_2 \in U$.

As a consequence of the lemma, if we are interested in the values of A_Ω^{-1} in a subset U of the possibly infinite volume Ω, it is sufficient to invert A on a suitable *larger* subset V, with $V \subset \Omega$. Quite generally, the functions of interest have the property $A_\Omega^{-1}(\mathbf{r}_1,\mathbf{r}_2)\to 0$ as $|\mathbf{r}_1-\mathbf{r}_2|\to\infty$. Therefore, the hypothesis of the lemma can be regarded as true to any degree of accuracy, for a large enough set V.

APPENDIX B: ANALYTIC CONTINUATION OF FREQUENCY INTEGRALS

The presence of nonanalyticities close to the contour of frequency integration renders it difficult to integrate expressions containing the Green function G and the effective potential W numerically, as for the polarization [Eq. (4)] or the self-energy [Eq. (6)]. Consider the integral in Eq. (4) first. The Green function has poles (or cuts) just below the real ω axis for $\omega > \mu$ and above for $\omega < \mu$. Therefore, if z is a pole or a point in the cut, $\mathrm{sgn}(\mu - \mathrm{Re}\, z) = \mathrm{sgn}(\mathrm{Im}\, z)$. Note that the factor $e^{i\omega'\eta}$ means that only the residues related to occupied states ($\omega < \mu$) are summed. To avoid the numerical difficulty, one can define the analytic continuation of P to complex frequencies as the sum over the same residues, now evaluated at the complex frequency.[24] It is easy to show that in the case of purely imaginary frequencies this corresponds to rotate the integration contour to the complex frequency axis $\mu + iu'$ (u,u' real). In the GWA the continued polarization is

$$P_0(iu) = -2i\int_{\mu-i\infty}^{\mu+i\infty} d\omega' G_0(\omega'+iu)G_0(\omega'). \quad \text{(B1)}$$

On the same footing, also the self-energy [Eq. (6)] can be continued to complex frequencies. If $\omega = \mu + iu$, the following relation holds:

$$\Sigma_0(\mu+iu) = i\int_{-i\infty}^{i\infty} d\omega' G_0(\omega'+\mu+iu)W_0(\omega'), \quad \text{(B2)}$$

where the analytic continuation of $W_0(\omega' = iu')$ is evaluated by inserting $P_0(iu)$ into Dyson's equation. Note that the Lehmann representation of P_0 implies that a pole z of W_0 has $\mathrm{sgn}(\mathrm{Im}\, z) = -\mathrm{sgn}(\mathrm{Re}\, z)$.

The self-energy resulting from Eq. (B2) will be known on the complex line $\omega = \mu + iu$. This is useful for the evaluation of integral properties (e.g., the total energy), but for spectral properties the Green function (and hence the self-energy) has to be evaluated at real frequencies. To this end, one can fit Σ_{XC} on the complex axis with a simple analytic expression, to be continued to the real axis.[25] The multipole one is perhaps the more common:

$$\Sigma_{\mathrm{XC}}(\omega) = a_0 + \sum_{j=1}^{N} \frac{b_j}{\omega - c_j}. \quad \text{(B3)}$$

A small number of poles ($N = 2 \sim 4$) normally provides a good fit.

To rotate the integration path in frequency space we recall the following useful result. Consider the two integrals, where ω, a, and b are real:

$$F_1(\omega) = \int_{-\infty}^{+\infty} d\omega' \frac{1}{(\omega' - z_1)(\omega + \omega' - z_2)}$$

$$= i\pi \frac{\mathrm{sgn}(\mathrm{Im}z_1) - \mathrm{sgn}(\mathrm{Im}z_2)}{\omega - z_2 + z_1}, \quad \text{(B4)}$$

$$F_2(\omega) = \int_{a-i\infty}^{a+i\infty} d\omega' \frac{1}{(\omega' - z_1)(b + i\omega + \omega' - z_2)}$$

$$= i\pi \frac{\mathrm{sgn}(a - \mathrm{Re}\, z_1) - \mathrm{sgn}(a + b - \mathrm{Re}\, z_2)}{b + i\omega - z_2 + z_1}. \quad \text{(B5)}$$

The two numerators are equal if $\mathrm{sgn}(\mathrm{Im}z_1) = \mathrm{sgn}(a - \mathrm{Re}z_1)$ and $\mathrm{sgn}(\mathrm{Im}z_2) = \mathrm{sgn}(a + b - \mathrm{Re}z_2)$. In this case: $F_2(\omega) = F_1(b + i\omega)$, i.e., F_2 is the analytic continuation of F_1 to complex frequencies $b + i\omega$. Notice that, to be analytic, the continuation has to be performed *after* the integration. If both z_1 and z_2 are poles of the time-ordered Green function [as for the polarization in Eq. (4)], it follows from the Lehmann representation that the condition is met for $a = \mu$ and $b = 0$. If z_1 is a pole of the effective interaction and z_2 is a pole of the time-ordered Green function [as for the self-energy in Eq. (6)], the condition is met for $a = 0$, $b = \mu$.

*Present address: SISSA/ISAS, via Beirut 4, I-34014 Trieste; Electronic address: fratesi@sissa.it

†Electronic address: gianpaolo.brivio@mater.unimib.it

‡Electronic address: luca.molinari@mi.infn.it

[1] L. Hedin, Phys. Rev. **139**, A796 (1965).

[2] W. G. Aulburg, L. Jönsson, and J. W. Wilkins, *Solid State Physics*, edited by H. Ehrenreich and F. Spaepen (Academic, New York, 2000), Vol. 54.

[3] F. Aryasetiawan and O. Gunnarsson, Rep. Prog. Phys. **61**, 237 (1998).

[4] M. L. Tiago, J. E. Northrup, and S. G. Louie, Phys. Rev. B **67**, 115212 (2003).

[5] A. G. Eguiluz, M. Heinrichsmeier, A. Fleszar, and W. Hanke, Phys. Rev. Lett. **68**, 1359 (1992).
[6] G. Onida, L. Reining, and A. Rubio, Rev. Mod. Phys. **74**, 601 (2002).
[7] G. P. Brivio and M. I. Trioni, Rev. Mod. Phys. **71**, 231 (1999).
[8] S. Brodersen and W. Schattke, Phys. Rev. B **66**, 153303 (2002).
[9] W. Kohn, Phys. Rev. Lett. **76**, 3168 (1996).
[10] W. Kohn and A. E. Mattsson, Phys. Rev. Lett. **81**, 3487 (1998).
[11] P. G. Gonzàlez and R. W. Godby, Phys. Rev. Lett. **88**, 056406 (2002).
[12] G. Fratesi, G. P. Brivio, P. Rinke, and R. W. Godby, Phys. Rev. B **68**, 195404 (2003).
[13] B. Holm and U. von Barth, Phys. Rev. B **57**, 2108 (1998).
[14] J. E. Inglesfield, J. Phys. C **14**, 3795 (1981).
[15] J. E. Inglesfield and G. A. Benesh, Phys. Rev. B **37**, 6682 (1988).
[16] M. I. Trioni, G. P. Brivio, S. Crampin, and J. E. Inglesfield, Phys. Rev. B **53**, 8052 (1996).
[17] C. Menchini, M. I. Trioni, and G. P. Brivio, Phys. Rev. B **67**, 035408 (2003).
[18] J. F. Dobson, *Density Functional Theory*, Vol. 337 of NATO ASI Series B: Physics, edited by E. K. U. Gross and R. M. Dreizler (Plenum, New York, 1995), p. 393.
[19] H. Ishida, Phys. Rev. B **57**, 4140 (1998).
[20] P. Sánchez-Friera and R. W. Godby, Phys. Rev. Lett. **85**, 5611 (2000).
[21] R. Matzdorf, Surf. Sci. Rep. **30**, 153 (1998).
[22] S. Schintke, S. Messerli, M. Pivetta, F. Patthey, L. Libioulle, M. Stengel, A. D. Vita, and W.-D. Schneider, Phys. Rev. Lett. **87**, 276801 (2001).
[23] H. Ishida, Phys. Rev. B **63**, 165409 (2001).
[24] R. W. Godby, M. Schlüter, and L. J. Sham, Phys. Rev. B **37**, 10 159 (1988).
[25] M. M. Rieger, L. Steinbeck, I. D. White, H. N. Rojas, and R. W. Godby, Comput. Phys. Commun. **117**, 211 (1999).